CrystEngComm

ROYAL SOCIETY OF CHEMISTRY

HIGHLIGHT

View Article Online
View Journal | View Issue

Cite this: *CrystEngComm*, 2025, **27**, 127

Exploring flexibility in molecular crystals: bending responses to light and mechanical stress

Sotaro Kusumoto *[a] and Yang Kim[b]

Received 7th November 2024,
Accepted 20th November 2024

DOI: 10.1039/d4ce01131g

rsc.li/crystengcomm

Crystalline materials are traditionally known for their brittleness when subjected to external stress. However, recent advancements have enabled the creation of flexible crystals through specific molecular architectures. These innovative materials can deform in response to light or mechanical stress, making them promising candidates for smart materials, sensors, actuators, and optoelectronic devices. While considerable research has been conducted on the effects of individual external stresses, the investigation of flexible crystals that respond to multiple stimuli and their bending mechanisms remains to be improved. This review aims to elucidate the mechanisms that govern the flexibility of crystals responsive to both light and mechanical stimuli. We will analyze the mechanical properties related to 1D or 2D assembly, [2 + 2] or [4 + 4] photodimerization, and molecular isomerization and provide insights on designing new molecular structures to enhance the flexibility of crystals. Additionally, we will address current challenges in the field and propose future research directions to advance the development of flexible molecular crystals.

1. Introduction

Molecular crystals exhibit a range of mechanical responses, including movement, bending, jumping, bursting, and twisting,[1] to various external stimuli such as heat,[2] light,[3] mechanical force,[4] humidity,[5] vapor,[6] and magnetic fields,[7] and have recently garnered significant attention for potential applications in artificial muscles[8] and actuation devices.[9] However, molecular crystals exhibiting reversible or irreversible bending in response to both light and mechanical stress are relatively rare.[10] This scarcity often arises from unpredictable changes in physical properties or from undesired chemical reactions triggered by external stimuli. Multi-stimuli responsive materials—molecular crystals responding to two or more distinct stimuli—offer enhanced versatility. While such materials have been reported,[11] they remain infrequent. This review highlights recent progress in dual-responsive molecular crystals that undergo deformation under mechanical force and light. Since pioneering studies on elastic crystals, such as caffeine cocrystals[12] and $Cu(acac)_2$ complexes,[13] and plastic crystals, such as hexachlorobenzene,[14] significant research[12–14] has focused on crystals where weak intermolecular interactions (*e.g.*, van der Waals forces) are influenced by external stress. These interactions can lead to microscopic molecular slippage resulting in macroscopic changes, including elasticity,[15] plasticity,[16] superelasticity,[17] ferroelasticity,[18] and superplasticity.[19] Elastic deformation has been achieved using π-conjugated molecules to promote π–π stacking interactions,[3c,15a,d,h–j] whereas plastic deformation can be induced by introducing halogen groups or long alkyl chains to create 2D sliding planes.[14,15h,16c–e,g,h] Despite numerous studies on organic compounds and metal complexes, examples of materials responding to stimuli beyond mechanical forces remain limited.

Photoreactive sites are crucial for inducing significant changes in molecular crystals through light irradiation. Many studies focus on photoswitchable materials utilizing *E* (*trans*) ⇌ *Z* (*cis*) isomerization of compounds containing –N=N– (ref. 20) or –C=N– moieties,[21] photoreactions of diarylethenes,[22] [4 + 4] photodimerization of anthracenes,[23] and [2 + 2] cycloaddition of olefins.[24] However, light irradiation often leads to fracturing or cracking in crystals undergoing these photoreactions, limiting their suitability for studying bendable properties. Therefore, exploring additional crystals capable of efficient bending under light irradiation is crucial. Designing dual-responsive molecular crystals that respond to mechanical force and light requires incorporating molecules that respond independently or concurrently to each stimulus.

This review focuses on recent advances in molecular crystals responsive to external stress, particularly those based on acylhydrazone and azobenzene derivatives, and those containing olefins or anthracene moieties (Fig. 1, Table 1).

[a] *Department of Material and Life Chemistry, Faculty of Engineering, Kanagawa University, 3-27-1 Rokkakubashi, Kanagawa-ku, Yokohama 221-8686, Japan. E-mail: kusumoto@kanagawa-u.ac.jp*
[b] *Department of Chemistry, Graduate School of Science and Technology, Kumamoto University, 2-39-1 Kurokami, Chuo-ku, Kumamoto 860-8555, Japan*

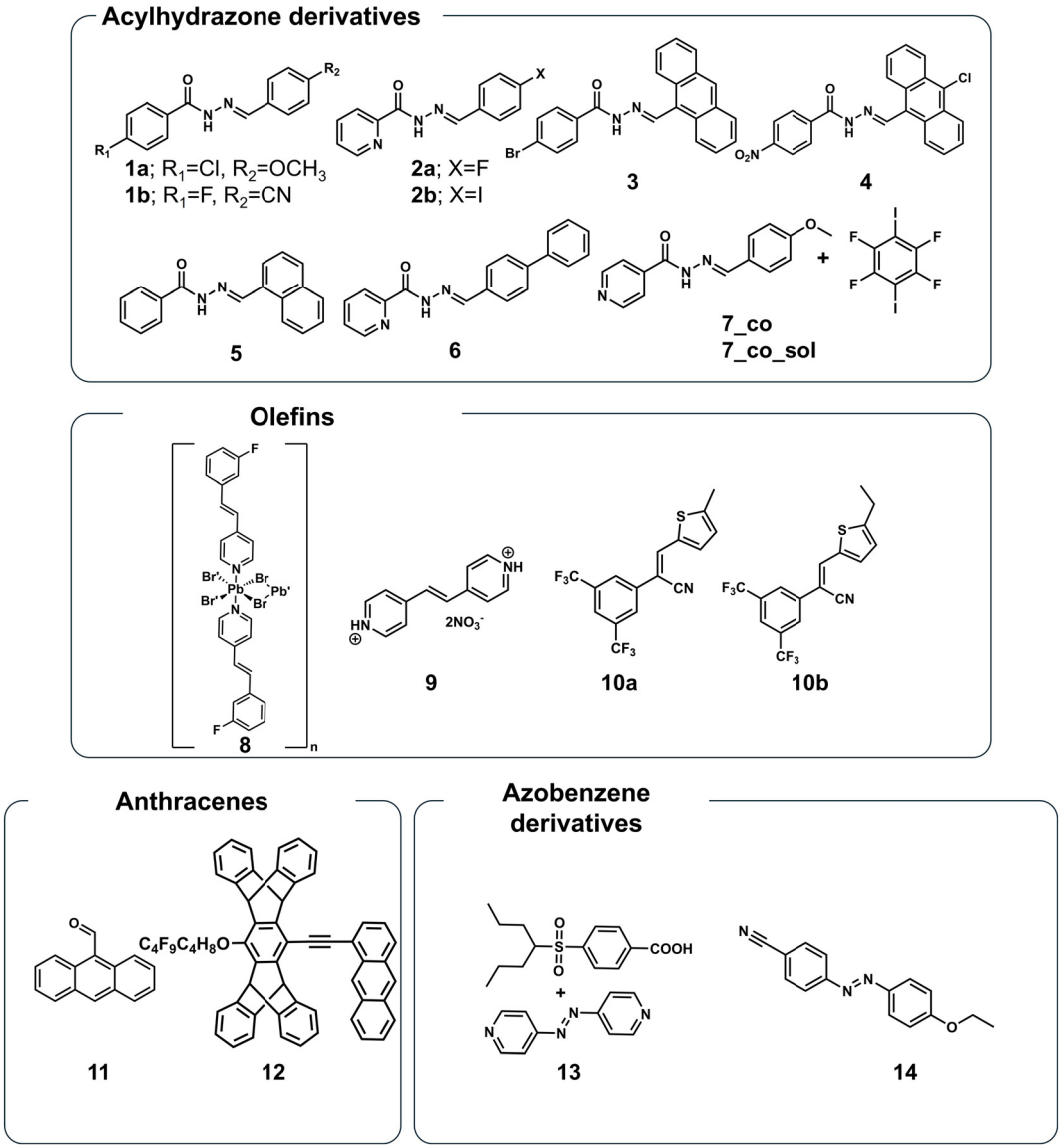

Fig. 1 Chemical structures of the crystals that respond to external stresses discussed in this review.[11]

2. Acylhydrazone derivatives

Acylhydrazones, incorporating the –C═N–N– moiety, exhibit *E*–*Z* photoisomerization,[21a] a property that underpins their use as molecular photoswitches. Their straightforward synthesis and high stability have spurred extensive investigation. However, the mechanical response of acylhydrazone crystals to external stress has received comparatively less attention until recently. Nath *et al.*[11a] first reported (2019) on the light- and mechanically-induced responses of needle-shaped photoswitchable acylhydrazone derivatives (**1a** and **1b**), which were synthesized from aromatic aldehydes and the corresponding hydrazides. UV-vis spectroscopy of **1a** in acetonitrile revealed two absorption maxima at 226 nm and 316 nm. UV irradiation increased absorbance at 226 nm and decreased absorbance at 316 nm, consistent with *E* → *Z* photoisomerization. This photoisomerization was confirmed by irradiating a single crystal with UV light from a Hg–Xe lamp (Fig. 2a). Following UV irradiation, both **1a** and **1b** exhibited bending, which was reversed upon heating to 40 °C, restoring crystallinity and returning the crystals to their original straight form *via* thermal *Z* → *E* isomerization. Furthermore, applying force with tweezers to the crystal center resulted in irreversible plastic deformation for **1a** (Fig. 2b) but reversible elastic deformation for **1b** (Fig. 2c).

Single-crystal X-ray diffraction analysis revealed that **1a** contains water molecules and exhibits weak Cl···O interactions along the *c*-axis. This facilitates plastic deformation due to the arrangement of molecules in slip planes with weak intermolecular interactions parallel to the (001) plane (Fig. 2d).[14] In contrast, **1b**, a monohydrate crystal, forms O–H···O hydrogen bonds along the *a*-axis between the C═O group and water molecules, and N–H···O hydrogen

Table 1 A summary table of the mechanical characteristics for each compound

Compounds	Bending type	Maximum elastic strain (ε_{max}) (%)	Young's modulus (E), measured by three-point bending test (GPa)	Reduced modulus (Er), measured by nanoindentation test (GPa)	Hardness (H), measured by nanoindentation test (GPa)
1a (ref. 11*a*)	Plastic	—	—	—	—
1b (ref. 11*a*)	Elastic	—	—	—	—
2a (ref. 11*b*)	Elastic	0.5	—	4.10 ± 0.14	0.20 ± 0.01
2b (ref. 11*b*)	Elastic	0.7	—	—	—
3 (ref. 11*c*)	Elastic	3.5	—	—	—
4 (ref. 11*d*)	Elastic	3.3	—	—	—
5 (ref. 11*e*)	Elastic	2.7			
6 (ref. 11*f*)	Elastic			0.211 ± 0.057	0.045 ± 0.007
7_co (ref. 11*g*)	2D elastic	2.2 (001) 1.4 (010)	—	—	—
7_co_sol (ref. 11*g*)	2D elastic	1.9 (001) 1.2 (100)	—	—	—
8 (ref. 11*h*)	Elastic	1.3	—	—	—
9 (ref. 11*i*)	Elastic	2.4	1.18	—	—
10a (ref. 11*j*)	Plastic	—	4.51	4.29 ± 0.20	0.12 ± 0.01
10b (ref. 11*j*)	Elastic	>1	1.04	6.91 ± 0.12	0.21 ± 0.01
11 (ref. 11*k*)	2D elastic	6.8 (001) 6.3 (010)		6.74 ± 0.15 (001) 6.31 ± 0.08 (010)	0.14 ± 0.007 (001) 0.13 ± 0.005 (010)
12 (ref. 11*l*)	Elastic	12.4		0.320 ± 0.014 (100) 2.657 ± 0.017 (001)	0.031 ± 0.001 (100) 0.205 ± 0.001 (001)
13 (ref. 11*m*)	Elastic	—	—	—	—
14 (ref. 11*n*)	2D elastic			0.00542 ± 1.88	0.00174 ± 0.45

bonds along the *b*-axis between the acylhydrazone N–H groups and water molecules. The anisotropic nature of this hydrogen bonding network resembles that observed in highly flexible elastic crystals such as $Cu(acac)_2$.[13] Subsequent studies demonstrated that modifying substituents can tune the resulting crystal properties, yielding materials that exhibit predominantly elastic or plastic behavior in response to light. However, these studies generally lack quantitative mechanical characterization (*e.g.*, three-point bending tests, nanoindentation), limiting a comprehensive understanding of the materials' full mechanical capabilities. Further experiments are needed to fully elucidate the potential for enhanced mechanical flexibility beyond that observed in conventional molecular crystals.

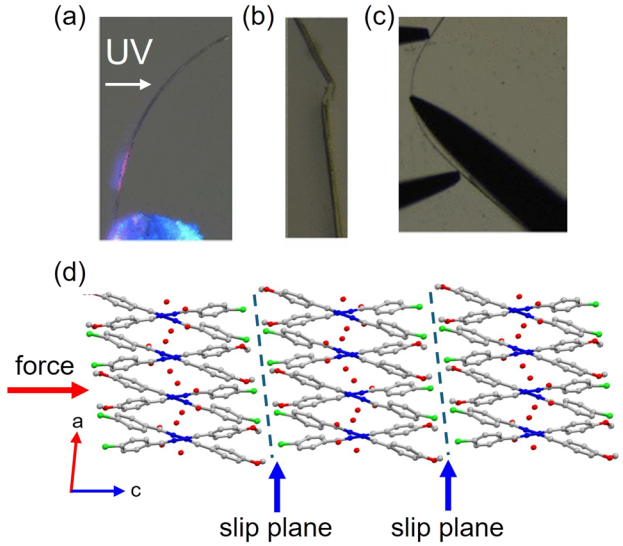

Fig. 2 (a) Crystal **1a** under UV irradiation. (b) Plastic bending of **1a** by application of pressure on the (001) face. (c) Elastic bending of **1b**. (d) The packing structure viewed down the *b*-axis. Slip planes for plastic bending were observed along the *c*-axis. Reproduced from ref. 11*a* with permission from the American Chemical Society, copyright 2019.

In 2021, J. Jia *et al.*[11b] reported on the elastic deformation and photo-induced bending behavior of acylhydrazone derivative crystals synthesized from 4-fluorobenzaldehyde (**2a**) or 4-iodobenzaldehyde (**2b**) and 2-pyridinecarboxylic acid hydrazide (Fig. 3a). Exposure to UV light (365 nm) initially caused bending away from the light source, but continued irradiation reversed this, resulting in bending towards the light source. Heating to 80 °C restored the original straight shape. UV-vis and ^{1}H NMR spectroscopic analysis, performed before and after UV irradiation, revealed that $E \rightarrow Z$ isomerization, initially predominant on the crystal surface facing the light source, drives this bending behavior. Prolonged irradiation induces $Z \rightarrow E$ reverse isomerization and structural relaxation due to thermal effects, thus altering the bending direction. Both **2a** and **2b** crystals exhibited stress-induced deformation (Fig. 3b), with maximum elastic strains of 0.5% and 0.7%, respectively—lower than those reported for other elastic crystals.[15] Nanoindentation measurements on the bent surface **2a** yielded an elastic modulus of 4.10 ± 0.14 GPa and a hardness of 0.20 ± 0.01 GPa. Single-crystal X-ray diffraction analysis revealed a chain-like structure formed *via* hydrogen bonds (C–H···N, N–H···O, C–H···O) and C–H···π interactions within the (1$\bar{0}$1) plane (Fig. 3c). The distances of these weak supramolecular interactions are tunable under external stress, influencing intermolecular distances and leading to elastic deformation.

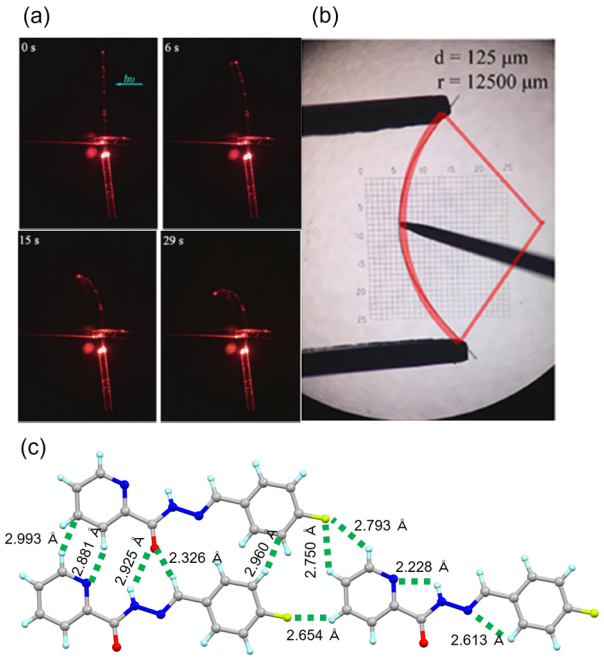

Fig. 3 (a) Photo-bending behavior and passive light output direction control. (b) Elastic bending. (c) Intermolecular interactions of **2a**. Reproduced from ref. 11*b* with permission from the Elsevier, copyright 2021.

These interactions effectively dissipate intermolecular binding energy, acting as "structural buffers" and preventing crystal fracture. Fig. 3a shows that needle-shaped crystal **2a** transmits 635 nm light, with a red dot at the crystal tip marking the emission point. UV irradiation induces bending, shifting this red dot and allowing for control over the direction of passive light transmission, demonstrating the potential for light-controlled manipulation of light transmission.

Recent studies demonstrate that the crystals of anthracene derivatives, particularly those incorporating an acylhydrazone moiety (compounds **3** and **4**),[11c,d] exhibit bending in response to both optical and mechanical stimuli. Compound **3**, a yellow, needle-shaped crystal synthesized *via* condensation of 4-bromobenzhydrazide and 9-anthraldehyde,[11c] displays significant flexibility, readily bending under external stress to achieve a maximum elastic strain of approximately 3.5%. Single-crystal X-ray diffraction reveals a structure stabilized by supramolecular interactions, including C–H···π, C–H···O, and C–H···Br interactions. These interactions organize the molecules into layers within the *bc* plane, which are stacked along the *a*-axis (the crystal growth direction) *via* π–π interactions (4.332 Å). This cross-shaped packing motif generates numerous weak, dispersive interactions, resulting in an interlocking structure that facilitates short-range molecular movement and contributes to the crystal's elasticity. Photoisomerization ($Z \rightarrow E$) induces reversible bending, with the original state ($E \rightarrow Z$) restored upon heating. This reversibility was confirmed through solution UV-vis and ^{1}H NMR spectroscopy.

Crystal **4**, synthesized from 4-nitrobenzhydrazide and 10-chloro-9-anthraldehyde, exhibits a similar structure to **3** and displays elastic deformation with a maximum strain of 3.3%.[11d] This suggests that the light-induced bending observed in these compounds arises from $E \rightarrow Z$ isomerization.

The (*E*)-*N*-(naphthalene-1-ylmethylene)benzohydrazide crystal (**5**)[11e] exhibits a notable mechanical response to external stress. The crystal structure features N–H···O ($d_{H\cdots O}$ = 2.04 Å, $D_{N\cdots O}$ = 2.909(3) Å, $\theta_{N-H\cdots O}$ = 171°) and C–H···O (2.68 Å, 3.426(4) Å, 139°) hydrogen bonds along the *a*-axis, as well as π–π interactions between benzene and naphthalene rings (inter-ring centroid-to-centroid distances of 3.381 Å and 3.716 Å, respectively). The molecules are densely packed in a 3D coordinated network of energetically equivalent intermolecular interactions. Applying pressure to the (001) plane with a needle induces bending into a loop without fracture, demonstrating a maximum elastic strain of 2.7%. The crystal fully recovers its original shape upon removal of the applied force. Furthermore, attaching a single crystal to a metal needle and irradiating it with UV light also results in bending. Heating the bent crystal at 65 °C for 1 hour reverses the bending, attributed to $E \rightleftharpoons Z$ isomerization.

J. Peng *et al.*[11f] demonstrated that (*E*)-*N*′-([1,1′-biphenyl]-4-ylmethylene)picolinohydrazide (**6**) exhibits reversible elastic deformation under external stress, suggesting its potential as an optical waveguide. This crystal structure is defined by a network of supramolecular interactions, including C–H···O (2.293 Å), C–H···N (2.907 Å), and C–H···π (3.309 Å, 3.830 Å) interactions within the (100) plane, and C–H···O (2.579 Å and 2.293 Å) interactions within the (002) plane (parallel to the *c*-axis). Upon exposure to UV light (365 nm, 3 W), the crystal rapidly bends away from the light source (Fig. 4a). Heating a UV-bent sample to 120 °C reversed the bending. ^{1}H NMR spectroscopy confirmed that $E \rightarrow Z$ isomerization occurs under UV irradiation, and the reverse ($Z \rightarrow E$) isomerization upon heating. The crystal exhibits reversible elastic deformation when an external force is applied and released along the (002) plane (Fig. 4b). Nanoindentation measurements on the (002) plane yielded an elastic modulus of 0.211 ± 0.057 GPa and a hardness of 0.045 ± 0.007 GPa, indicating good elastic properties. The numerous supramolecular interactions within the (100) plane likely facilitate energy dissipation during bending. Upon release of the external force, these interactions return to their original state, enabling recovery of the initial crystal shape. Further experiments investigated the control of passive light transmission using both light and mechanical stimuli (Fig. 4c and d). Fixing the crystal with adhesive and introducing light (635 nm) at one end generated a distinct red spot at the crystal edge, demonstrating light transmission. UV irradiation or mechanical force induced bending, shifting the red spot and thus manipulating the direction of passive light transmission.

T. Wang *et al.*[11g] synthesized an acylhydrazone derivative, MBINH, from isonicotinohydrazide and

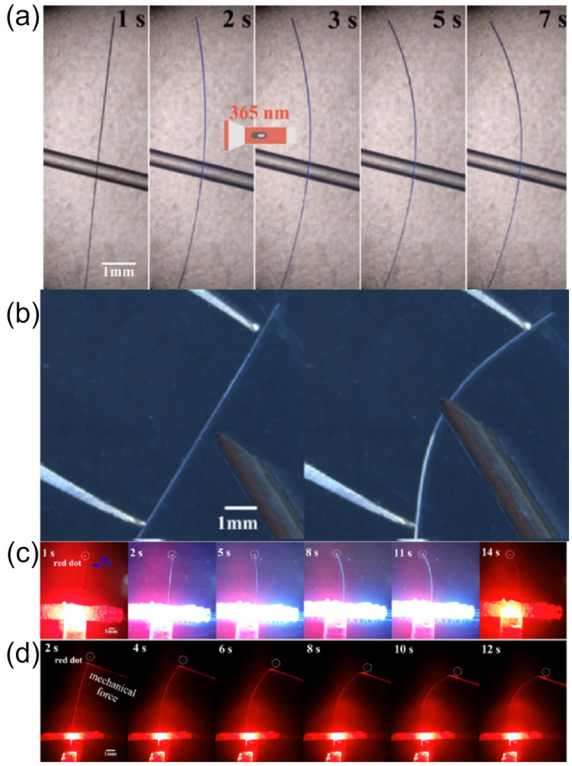

Fig. 4 (a) Photographic images of crystal **6** driven by UV light. (b) Photographic images of the elastic bending. Passive light (635 nm) output images of the long crystal under 365 nm light (c) and mechanical force (d). Reproduced from ref. 11*f* with permission from the Royal Society of Chemistry, copyright 2024.

4-methoxybenzaldehyde. They then prepared a 2 : 1 cocrystal (**7_co**) of MBINH and tetrafluoro-3,6-diodobenzene (TFDI) to investigate its mechanical response (Fig. 5a). MBINH crystals

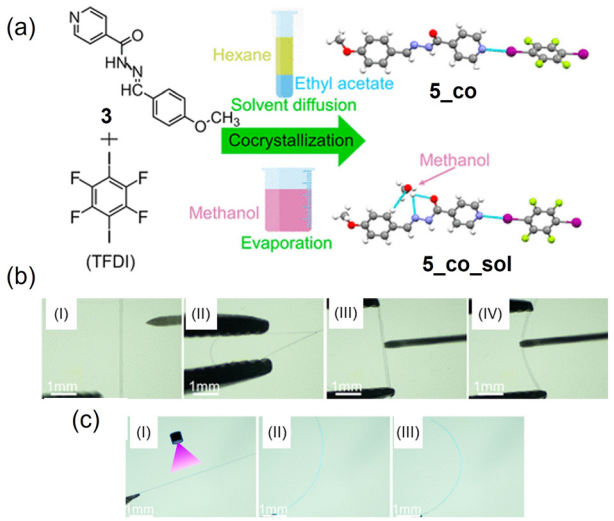

Fig. 5 (a) Illustration of the formation of **7_co** and **7_co_sol**. (b) Elastic bending of **7_co** crystals along the prominent crystal face (001) (I–II) and minor crystal face (001) (III–IV). (c) Photo-induced bending of **7_co**. Reproduced from ref. 11*g* with permission from the American Chemical Society, copyright 2023.

(7) alone proved brittle under mechanical stress, exhibiting a maximum elastic strain of only ~0.3%. In contrast, cocrystals solvated with methanol (**7_co_sol**), obtained by recrystallization of **7_co** from methanol, demonstrated significant elastic deformation (Fig. 5b). Both **7_co** and **7_co_sol** exhibited 2D elastic bending, withstanding twisting without fracture. The maximum elastic strains were 2.2% and 1.4% for **7_co**, and 1.9% and 1.2% for **7_co_sol**, comparable to values reported for other elastic crystals.[15*f–h*] Single-crystal X-ray diffraction analysis revealed a 2 : 1 MBINH : TFDI stoichiometry in **7_co** and a 1 : 1 : 1 MBINH : TFDI : methanol stoichiometry in **7_co_sol**. In both cocrystals, the electrophilic iodine atoms of TFDI interact with the pyridyl nitrogen atoms *via* C–I···N halogen bonds. The bending mechanism in **7_co** involves numerous weak intermolecular interactions, including π-stacking and a herringbone molecular arrangement. A similar combination of π-stacking and herringbone arrangements in **7_co_sol** creates a wave-like pattern that facilitates elastic deformation. UV irradiation (365 nm) induced bending in **7_co** towards the light source, forming a semicircular arc (Fig. 5c). However, **7_co_sol** showed only slight bending before cracking, likely due to its lower flexibility and inability to effectively dissipate internal stress generated during UV irradiation. Heating **7_co** to 100 °C reversed the light-induced bending; however, **7_co_sol** did not fully recover its original shape due to methanol evaporation during heating, resulting in crystal fracture. ^{1}H NMR spectroscopy, performed before and after UV irradiation, confirmed that *E–Z* isomerization drives the light-induced bending in **7_co**.

3. [2 + 2] cycloaddition reactions of olefins

The [2 + 2] photodimerization of olefins offers a valuable approach for creating dual-responsive crystals exhibiting both light- and mechanically-induced bending. This responsiveness arises from macroscopic changes in crystal behavior driven by photochemical reactions within the crystal. According to Schmidt's criterion,[25] photodimerization requires an inter-olefin distance of less than 4.2 Å. This constraint can be satisfied through careful molecular design.[26]

J. J. Vital *et al.*[11*h*] reported on the crystal of [$PbBr_2$(3F-spy)$_2$] (**8**), where 3F-spy represents 3-fluoro-4′-styrylpyridine. This crystal exhibits both elastic deformation and photo-induced bending. It forms a 1D coordination polymer along the *a*-axis, consisting of Pb(μ-O)$_2$Pb chains interconnected by bridging bromides and adjacent Pb(II) ions (Fig. 6a). The 3F-spy ligands coordinate to Pb(II) in a *trans* configuration along the *b*-axis and are arranged parallel. This 1D polymer network is further interconnected *via* crystal elongation, stabilized by supramolecular interactions, such as C–H···F and C–H···Br(Pb), oriented perpendicular to the *a*-axis. These interactions prevent slippage and plastic deformation under external stress. Applying a force to the (001) plane of a fixed

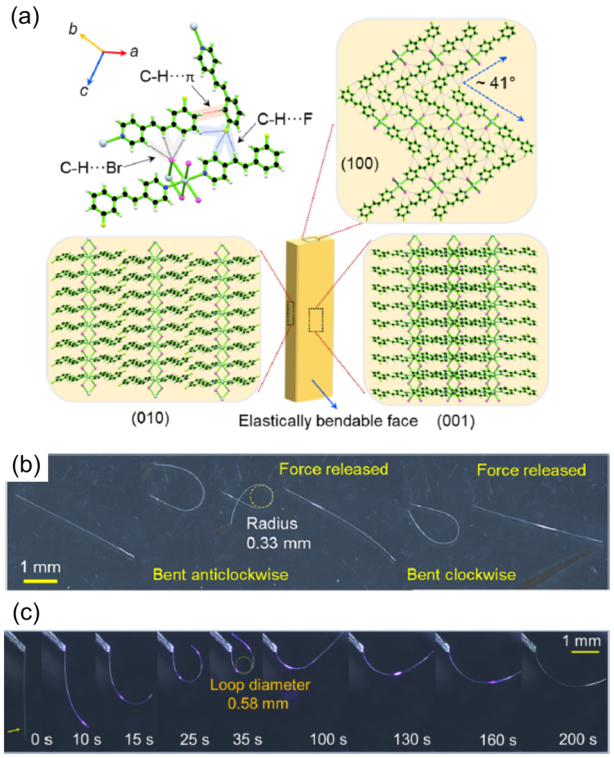

Fig. 6 (a) Crystal structure with weak interactions and packing viewed perpendicularly. (b) Elastic bending of single crystal **8** under external force. (c) Photo-induced bending of the crystal. Reproduced from ref. 11*h* with permission from the American Chemical Society, copyright 2021.

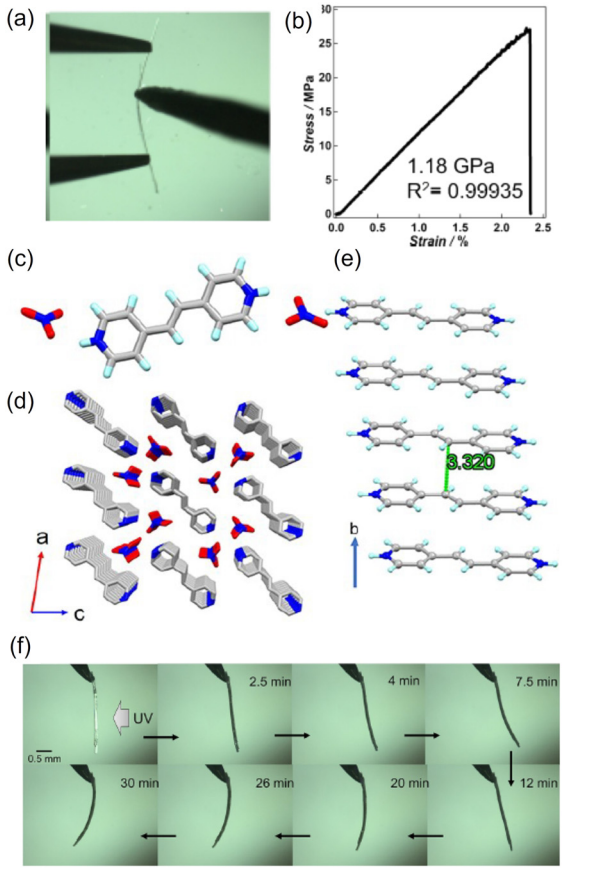

Fig. 7 (a) Crystal structure of **9**. (b) Packing arrangement viewed down the *b*-axis. (c) 1D arrangement of Ebpe molecules. (d) Stress-induced crystal bending. (e) Stress–strain curve in a three-point bending test. (f) Photoinduced crystal bending when exposed to UV light from the right side for up to 30 min.

crystal induced flexible bending with a maximum elastic strain of 1.3% (Fig. 6b). The crystal recovered its original shape upon removal of the external force. At 295 K, the distance between the olefin moieties of the 3F-spy ligand is 4.175 Å, close to the 4.2 Å limit imposed by Schmidt's criterion[25] for [2 + 2] photodimerization in the solid state. UV irradiation (360 nm) induced various photodynamic effects, including jumping, bending (Fig. 6c), and splitting, attributed to the formation of a cyclobutane ring *via* [2 + 2] photodimerization within the styryl moiety of the 3F-spy ligand. This effect diminished after a few minutes due to the termination of the dimerization reaction. The [2 + 2] cycloaddition reaction is the driving force behind the observed photomechanical effect, as confirmed by the formation of *rctt*-1,2-bis(4′-pyridyl)-3,4-bis(3′-fluorophenyl) cyclobutane (*rctt*-3F-ppcb; *rctt* denotes *regio-cis*, *trans*, *trans*) identified *via* ^{1}H NMR spectroscopy of the dissolved crystal residues in DMSO-d_6.

Because organic ionic salts exhibiting deformation in response to multiple external stimuli are rare, our group reported on the $[H_2Ebpe](NO_3)_2$ crystal (**9**), where H_2Ebpe represents (*E*)-1,2-bis(pyridine-4-yl)ethylene.[11*i*] This material is deformable under both mechanical force and UV light. Applying force with tweezers to a ~5 mm long crystal induced elastic deformation; the crystal returned to its original shape upon force removal (Fig. 7a). Three-point bending tests revealed an elastic modulus of 1.18 GPa (Fig. 7b), comparable to some soft polymers like nylon (2–5 GPa). Single-crystal X-ray diffraction revealed a 1D slip-stack structure (Fig. 7c–e). Previous studies have shown that 1D arrangements in crystals with π-conjugated systems often contribute to high flexibility.[3*c*,15*a*,*d*,*h*–*j*] The external force causes the expansion of π–π interactions in the outer arc and contraction in the inner arc, facilitating deformation. The inter-cation distance (3.320(2) Å) satisfies Schmidt's criterion[25] for [2 + 2] photodimerization. Alternating UV irradiation (365 nm) induced bending in response to the light direction (Fig. 7f), although this response diminished after a few cycles. The photodimerization of the olefin moieties in H_2Ebpe forms *rctt*-1,2,3,4-tetrakis(4-pyridiniumyl)cyclobutane, driving the light-induced deformation.

The mechanical responses of 5-methylthiophene-2-carbaldehyde (**10a**) and 5-ethylthiophene-2-carbaldehyde (**10b**) crystals were also investigated.[11*j*] Applying mechanical force to **10a** resulted in plastic deformation along the (010) plane, with no recovery upon force removal (Fig. 8a). The maximum elastic strain exceeded 1% regardless of crystal thickness. In contrast, **10b** exhibited reversible elastic

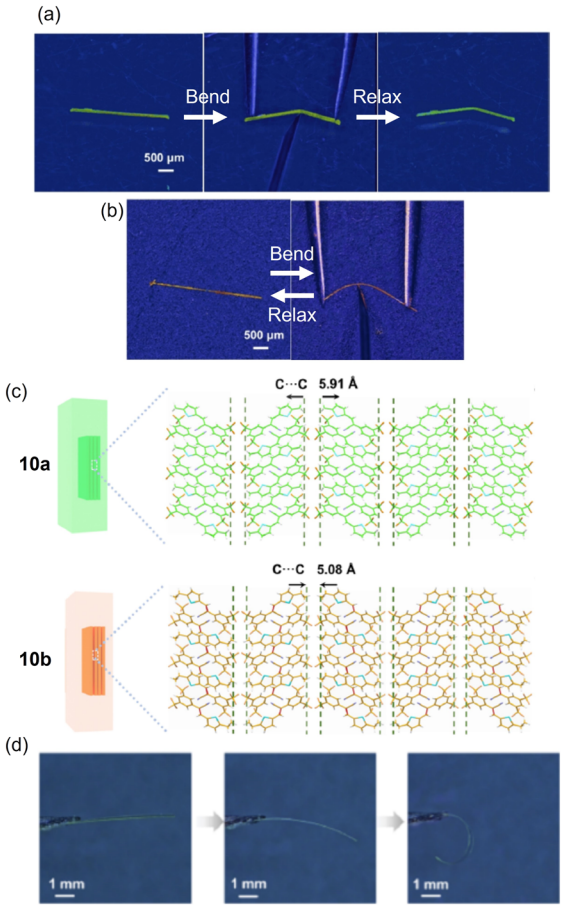

Fig. 8 (a) Plastic bending of **10a**. (b) Elastic bending of **10b**. (c) Packing arrangement of **10a** and **10b**. (d) Photoinduced bending of crystal **10a**. Reproduced from ref. 11*j* with permission from the American Chemical Society, copyright 2024.

deformation (Fig. 8b). Three-point bending tests measured Young's moduli of 4.51 GPa for **10a** and 1.04 GPa for **10b**. Nanoindentation tests yielded composite hardness (H) and elastic modulus (E) values of 0.12 ± 0.01 GPa and 4.29 ± 0.20 GPa for **10a**, and 0.21 ± 0.01 GPa and 6.91 ± 0.12 GPa for **10b**, indicating that **10b** is significantly harder. The nearly identical isotropic properties of both crystals suggest similar packing arrangements. Both crystals exhibit C–H···F and C–H···N interactions along the *a*-axis and C–H···F and F···C supramolecular interactions along the *b*-axis. However, the interlayer C···C distance differs: 5.91 Å for **10a** and 5.08 Å for **10b** (Fig. 8c). This shorter distance in **10b** suggests stronger intermolecular interactions, explaining the difference in mechanical behavior. Both crystals undergo [2 + 2] photocycloaddition upon light exposure. ^{1}H NMR spectroscopy and single-crystal X-ray diffraction analysis after light irradiation revealed light-induced deformation in **10a**, which was slower in **10b** (Fig. 8d). **10a** could be reversibly bent at least 30 times under UV irradiation, with bending less than 2°.

Reports on photo- and mechanically-deformable crystals utilizing [2 + 2] photodimerization remain scarce. As demonstrated in previous examples, a significant limitation of deformation caused by [2 + 2] cycloaddition is that the photochemically induced structural phase transition often leads to crystal degradation, thereby compromising reproducibility and reusability. Furthermore, slow [2 + 2] photodimerization can result in non-responsive crystals, highlighting the importance of reaction kinetics. Successful implementation of [2 + 2] photodimerization in photoresponsive, flexible crystals requires that the olefins satisfy Schmidt's criterion[25] and exhibit a fast reaction rate and adequate mechanical flexibility. The rarity of multi-reactive crystals undergoing [2 + 2] photodimerization can be attributed to these stringent requirements, the relatively short history of the photomechanical bending field, and the limited number of research groups focusing on this area. As a result, many of these reactions remain largely unexplored.

4. [4 + 4] cycloaddition reaction

Acenes, polycyclic aromatic hydrocarbons (PAHs) composed of three or more fused benzene rings, find applications in various fields, including p-type organic semiconductors. Their tendency towards close π–π stacking facilitates visible-light-induced [4 + 4] cycloaddition reactions, forming unique butterfly-like 3D dimers.[23] While photo-induced structural changes in acenes have been reported,[23] multi-stimuli responsive materials exhibiting stress-induced responses remain scarce.

H. Hao *et al.*[11k] reported on a 9-anthraldehyde crystal (**11**) exhibiting multiple stimuli-responsive properties, including

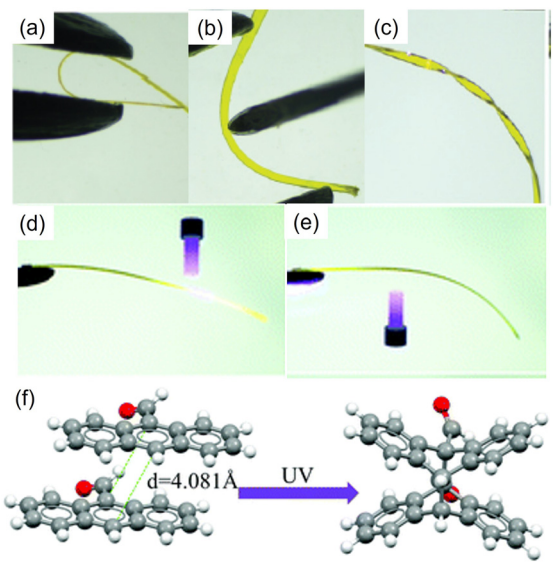

Fig. 9 (a) Elastic bending of crystal **11** by applying mechanical force on the (001) plane. (b) Elastic bending of crystal **11** by applying force on the (010) plane. (c) Elastic bending of the twisted crystal. (d and e) Optical microscopy images of photoinduced bending dependent on the direction of photoirradiation. (f) Schematic of the photodimerization reaction of **11**. Reproduced from ref. 11*k* with permission from the Royal Society of Chemistry, copyright 2021.

2D elastic bending, plastic twisting, and photo-induced bending. Applying mechanical force along the (001) direction readily induces bending into a loop, with full recovery upon force removal (Fig. 9a). Similar bending is observed along the (010) direction, enabling 2D elastic bending (Fig. 9b). Crystal **11** exhibits remarkably high maximum elastic strains of 6.8% and 6.3% along the (001) and (010) directions, respectively—significantly exceeding the typical critical elastic strain (~0.5%) for organic crystals. This exceptional 2D elasticity is attributed to the 1D π-stacked columns (3.63 Å interplanar spacing) along the *a*-axis, which can undergo spring-like compression and extension. The wave-like sheet stacking structure facilitated by weak C–H···π interactions further contributes to this elasticity. The unique 2D elastic bending also leads to plastic twisting (Fig. 9c). The crucial role of supramolecular interactions—specifically C–H···π and C–H···O interactions connecting the π-stacked columns—is evident in the elastic bending behavior: shear stress disrupts the crystal structure, creating new intermolecular interactions that allow for plastic deformation. Nanoindentation measurements yielded elastic moduli (E) and hardness values (H) of 6.74 ± 0.15 GPa and 0.14 ± 0.007 GPa along (001), and 6.31 ± 0.08 GPa and 0.13 ± 0.005 GPa along (010), respectively. These nearly isotropic values are consistent with the observed high elastic strain limits. In addition to its mechanical responsiveness, crystal **11** exhibits photoresponsiveness. Fixing one end of the crystal and irradiating it with UV light (365 nm, 500 mW cm^{-2}) induces rapid bending towards the light source (Fig. 9d and e). This behavior is attributed to a surface [4 + 4] photocycloaddition reaction (Fig. 9f), confirmed by ^{13}C NMR spectroscopy. However, this reaction is irreversible, precluding repeated actuation cycles.

J. S. Yang *et al.*[11l] reported on a semifluorinated octyloxy ($-OC_4H_8C_4F_9$)-substituted anthracene-acetylene-pentiptycene crystal (**12**) (Fig. 10a) exhibiting photoinduced elongation and elastic bending. This material displays green excimer fluorescence, undergoing elongation without fragmentation upon exposure to 419 nm light due to photodimerization. The fluorescence subsequently shifts to blue upon completion of the elongation process. The elongation varies from 11.0% to 21.6% depending on crystal length, while the width change ranges from 0.2% to 13.8%. The photodimerization efficiency is 94–97% (Fig. 10b). Notably, the [4 + 4] photodimer exhibits minimal visible light emission but reverts to monomers upon heating at 200 °C, recovering 71–78% of the original material. This process restores the green excimer fluorescence and the original crystal length (up to 51–93% recovery). Furthermore, irradiating crystal **12** from one side with 405 nm light causes bending away from the light source. Irradiating the opposite side reverses the bending direction, which can be repeated multiple times. The crystal exhibits a remarkable maximum elastic strain (ε) of 12.4%, approaching the maximum reported for organic crystals (14.6%)[15k] (Fig. 10c). Nanoindentation measurements on the (100) and (001) crystal faces yielded hardness values of 0.031 ± 0.001 GPa and 0.205 ± 0.001 GPa, and elastic moduli of 0.320 ± 0.014 GPa and 2.657 ± 0.017 GPa, respectively. Single-crystal X-ray diffraction reveals that anthracene units form supramolecular dimers (SDs) *via* π–π stacking (interplanar distance, d_c = 3.80 ± 0.01 Å) along the *b*-axis, creating 1D columns (Fig. 10a). These columns stack along the *a*-axis to form 2D π-stacked layers, which assemble along the *c*-axis to create a 3D crystal structure.

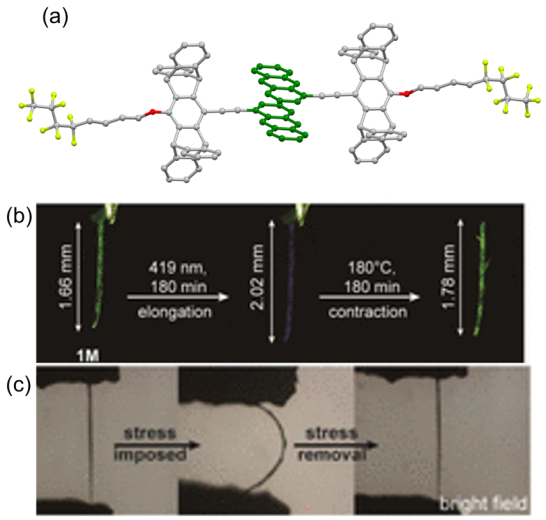

Fig. 10 (a) Crystal structure of compound **12**, showing interactions through π–π stacking with neighboring molecules. (b) Fluorescence images of photoinduced elongation and the subsequent thermal contraction. (c) Bending and unbending operations by a tweezer. Reproduced from ref. 11*l* with permission from the American Chemical Society, copyright 2023.

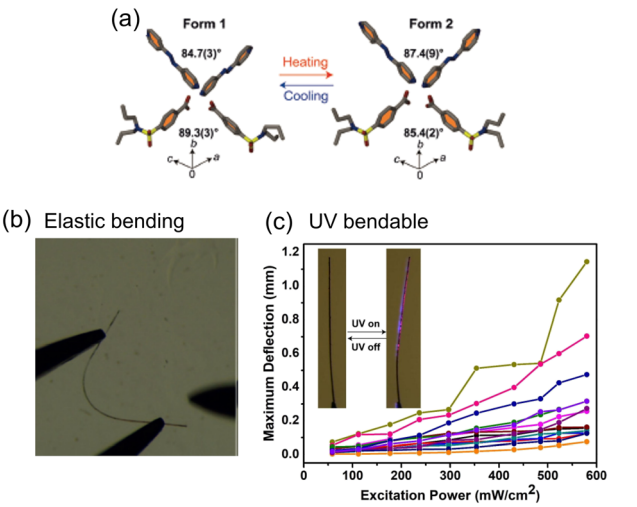

Fig. 11 (a) Subtle angle changes between the aromatic rings of two crisscrossed probenecid molecules and between the molecular planes of two crisscrossed azopyridine rings. (b) Slender crystals of **13** can be elastically bent. (c) Linear dependence of maximum deflection of the crystals on UV excitation power. Reproduced from ref. 11*m* with permission from the Wiley-VCH, copyright 2018.

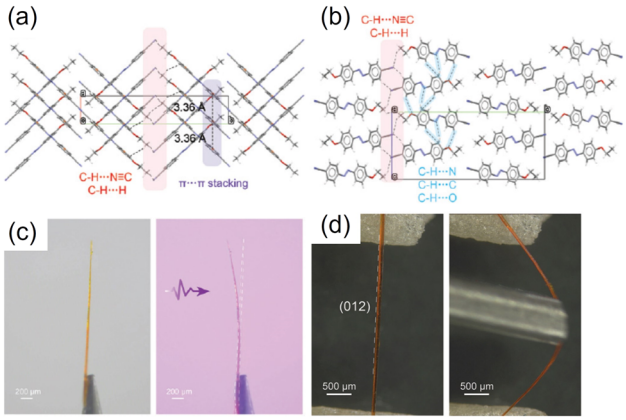

Fig. 12 (a and b) Crystal packing of **14**. (c) Photoinduced reversible deformation. (d) Elastic bending. Reproduced from ref. 11*n* with permission from the Royal Society of Chemistry, copyright 2021.

5. Azobenzene derivatives

Azobenzene derivatives are well-known photoresponsive molecules undergoing reversible *cis–trans* isomerization upon light exposure. Their unique properties have led to their widespread use in photoactuators and molecular switches.[20] While azobenzene-based crystals exhibiting light-induced bending have been reported, examples demonstrating significant mechanical responsiveness remain rare.

N. K. Nath *et al.*[11m] reported a 2:1 cocrystal (**13**) of probenecid and 4,4′-azopyridine (Fig. 11a), representing the first example of a smart crystalline material exhibiting reversible twisting, bending, and elastic deformation under multiple external stimuli (heat, UV light, and mechanical pressure) without fracture. Heating this cocrystal initiates a phase transition, with the phase front (habit plane) propagating at 62–64 °C. Cooling reverses this process. Single-crystal X-ray diffraction reveals that these phase transitions involve molecular rearrangements, specifically changes in the dihedral angle between the probenecid benzene ring and the azopyridine plane (Fig. 11a). The crystal undergoes anisotropic expansion (5.2% along the *a*-axis, 1.6% along the *b*-axis) and contraction (2.8% along the *c*-axis), resulting in twisting. Remarkably, fractured crystals of **13** exhibit self-healing upon heating near the phase transition temperature, suggesting that the phase transition facilitates this process. Applying mechanical pressure to **13** does not induce fracture but produces elastic bending, allowing the crystal to form a loop (Fig. 11b). The crystal structure features supramolecular interactions, including C═O···π, C–H···O, and van der Waals forces. Additional weak C–H···O interactions link the probenecid and azopyridine units, forming crossed 2D layers. This interlocked molecular packing, along with isotropic intermolecular interactions, is crucial for the elastic bending behavior. Importantly, the 4,4′-azopyridine moiety undergoes light-independent *trans–cis* isomerization upon UV irradiation, enabling rapid and reversible bending. The extent of bending increases with UV irradiation intensity (Fig. 11c). Even after prolonged UV irradiation (more than 10 minutes), the crystal retains its structural integrity, withstanding multiple actuation cycles. This remarkable behavior highlights the potential of azobenzene-based compounds for developing multifunctional materials responsive to multiple stimuli (light, heat, and mechanical force).

H. Hao *et al.*[11n] reported on a needle-shaped, polymorphic crystal of *trans*-4-cyano-4′-oxyethyl azobenzene (AzC_2) (**14**) synthesized *via* epitaxial crystallization. This multi-stimuli responsive material exhibits π–π stacking of AzC_2 molecules along the *a*-axis, with these columns interconnected *via* C–H···N, C–H···C, and C–H···O interactions along the *c*-axis, forming an interlocking 3D network (Fig. 12a). Further intermolecular interactions, specifically C–H···N≡C and C–H···H interactions, extend this network along the *b*-axis (Fig. 12b). Directing UV light onto the (012) crystal plane induces rapid bending towards the light source within one second, with immediate recovery to the original straight form upon cessation of irradiation (Fig. 12c). This reversible photomechanical bending is repeatable for at least 20 cycles without fatigue. Molecular dynamics simulations of the *trans* isomer indicate a 23.39% reduction in length, a 24.40% reduction in width, and a 10.34% increase in thickness, consistent with the observed deformation. Furthermore, applying external force perpendicular to the (012) plane or to the (020) plane induces elastic deformation (Fig. 12d), demonstrating 2D mechanical flexibility. Nanoindentation measurements revealed an elastic modulus of 5.42 ± 1.88 MPa and a hardness of 1.74 ± 0.45 MPa, highlighting this material's unusually soft mechanical properties.

Conclusions and outlook

This review has explored molecular crystals capable of deformation in response to both light and mechanical stress. These flexible crystals exhibit deformation under external mechanical force due to the arrangement of their constituent molecules into 1D or 2D arrays *via* supramolecular interactions. Crystals with suitable structural motifs, such as π-stacked columns or layered structures connected by elasticity-enhancing supramolecular interactions, readily undergo flexible deformation. The maximum elastic strains reported for the crystals discussed here range from 0.5% to 12.4%, with anthracene-functionalized compound **12** exhibiting exceptional flexibility. Crystals incorporating anthracene moieties show particular promise for developing light- and mechanically-responsive materials. The photoresponsive crystals reviewed here include acylhydrazone, azobenzene, olefin, and anthracene derivatives, with photoresponsiveness arising from mechanisms such as *E–Z* (*cis–trans*) isomerization and [2 + 2] or [4 + 4] photocycloaddition reactions. However, limited durability, often manifested as light-induced cracking, remains a significant challenge. Acylhydrazone and azobenzene derivatives offer improved repeatability in photo-

induced bending, although achieving large deformations remains difficult. While diarylethenes, extensively studied as photoswitches, have yet to be demonstrated as bendable crystals, their excellent reversibility and thermal stability make them attractive candidates for future development of durable, multi-stimuli responsive crystals. The relationship between mechanical flexibility and photo-induced bending in these crystals requires further investigation; however, enhancing crystal flexibility intuitively improves photo-induced bending. Addressing the challenges highlighted in this review—namely, improving durability and achieving larger deformations—will be crucial for advancing the fields of photoresponsive materials, molecular muscles, and actuators. Given the relative scarcity of reported examples, further research into plastic deformation in crystals is also warranted.

Data availability

All data used in this review are derived from previously published sources, which are cited in the reference list. No new data were created or analyzed in this study.

Conflicts of interest

There are no conflicts to declare.

Acknowledgements

This work was supported by KAKENHI Grant Number JP22K14698. This work was also supported by the Grant-in-Aid for Transformative Research Areas (A) "Supra-ceramics" (JSPS KAKENHI Grant Number JP23H04636).

References

1 P. Naumov, D. P. Karothu, E. Ahmed, L. Catalano, P. Commins, J. M. Halabi, M. B. Al-Handawi and L. Li, *J. Am. Chem. Soc.*, 2020, **142**, 13256–13272.

2 (*a*) P. Naumov, S. Chizhik, M. K. Panda, N. K. Nath and E. Boldyreva, *Chem. Rev.*, 2015, **115**, 12440–12490; (*b*) S. C. Sahoo, M. K. Panda, N. K. Nath and P. Naumov, *J. Am. Chem. Soc.*, 2013, **135**, 12241–12251; (*c*) K. Omoto, T. Nakae, M. Nishio, Y. Yamanoi, H. Kasai, E. Nishibori, T. Mashimo, T. Seki, H. Ito, K. Nakamura, N. Kobayashi, N. Nakayama, H. Goto and H. Nishihara, *J. Am. Chem. Soc.*, 2020, **142**, 12651–12657; (*d*) B. B. Rath, G. Gallo, R. E. Dinnebier, J. J. Vittal, B. B. Rath, G. Gallo, R. E. Dinnebier and J. J. Vittal, *J. Am. Chem. Soc.*, 2021, **143**, 2088–2096.

3 (*a*) P. Naumov, S. C. Sahoo, B. A. Zakharov and E. V. Boldyreva, *Angew. Chem., Int. Ed.*, 2013, **52**, 9990–9995; (*b*) R. Medishetty, S. C. Sahoo, C. E. Mulijanto, P. Naumov and J. J. Vittal, *Chem. Mater.*, 2015, **27**, 1821–1829; (*c*) R. Medishetty, A. Husain, Z. Bai, T. Runčevski, R. E. Dinnebier, P. Naumov and J. J. Vittal, *Angew. Chem., Int. Ed.*, 2014, **53**, 5907–5911.

4 (*a*) H. Liu, Z. Lu, Z. Zhang, Y. Wang and H. Zhang, *Angew. Chem., Int. Ed.*, 2018, **57**, 8448–8452; (*b*) S. Kusumoto, Y. Kim and S. Hayami, *Coord. Chem. Rev.*, 2023, **475**, 214890; (*c*) S. Hayashi and T. Koizumi, *Angew. Chem., Int. Ed.*, 2016, **55**, 2701–2704; (*d*) S. Ghosh and M. K. Mishra, *Cryst. Growth Des.*, 2021, **21**, 2566–2580; (*e*) W. Wu, K. Chen, T. Wang, N. Wang, X. Huang, Z. Wang and H. Hao, *J. Mater. Chem. C*, 2023, **11**, 2026–2052.

5 L. Lan, X. Yang, B. Tang, X. Yu, X. Liu, L. Li, P. Naumov and H. Zhang, *Angew. Chem., Int. Ed.*, 2022, **61**, e202200196.

6 X. Zheng, X. Liu, L. Liu, X. Li, S. Jiang, C. Niu, P. Xie, G. Liu, Z. Cao, Y. Ren, Y. Qin and J. Wang, *Angew. Chem., Int. Ed.*, 2022, **61**, e202113073.

7 X. Yang, L. Lan, L. Li, X. Liu, P. Naumov and H. Zhang, *Nat. Commun.*, 2022, **13**, 2322.

8 (*a*) S. M. Mirvakili and I. W. Hunter, *Adv. Mater.*, 2018, **30**, 1704407; (*b*) A. Buguin, M.-H. Li, P. Silberzan, B. Ladoux and P. Keller, *J. Am. Chem. Soc.*, 2006, **128**, 1088–1089.

9 (*a*) N. K. Nath, L. Pejov, S. M. Nichols, C. Hu, N. Saleh, B. Kahr and P. Naumov, *J. Am. Chem. Soc.*, 2014, **136**, 2757–2766; (*b*) Y.-X. Shi, W.-H. Zhang, B. F. Abrahams, P. Braunstein and J.-P. Lang, *Angew. Chem., Int. Ed.*, 2019, **58**, 9453–9458; (*c*) H. Koshima, R. Matsuo, M. Matsudomi, Y. Uemura and M. Shiro, *Cryst. Growth Des.*, 2013, **13**, 4330–4337.

10 (*a*) F. Terao, M. Morimoto and M. Irie, *Angew. Chem., Int. Ed.*, 2012, **51**, 901–904; (*b*) H. Wang, P. Chen, Z. Wu, J. Zhao, J. Sun and R. Lu, *Angew. Chem., Int. Ed.*, 2017, **56**, 9463–9467.

11 (*a*) P. Gupta, T. Panda, S. Allu, S. Borah, A. Baishya, A. Gunnam, A. Nangia, P. Naumov and N. K. Nath, *Cryst. Growth Des.*, 2019, **19**, 3039–3044; (*b*) J. Peng, J. Xing, J. Bai, Y. Ren, T. Wang and J. Jia, *Dyes Pigm.*, 2021, **194**, 109529; (*c*) D. Manoharan, S. Ahmad, F. Emmerling, B. Bhattacharya and S. Ghosh, *CrystEngComm*, 2023, **25**, 3237–3244; (*d*) M. Lakshmipathi, A. I. Sk, P. K. Kundu, S. Tothadi and S. Ghosh, *Cryst. Growth Des.*, 2023, **23**, 4939–4945; (*e*) P. J. Hazarika, P. Gupta, S. Allu and N. K. Nath, *CrystEngComm*, 2024, **26**, 1671–1676; (*f*) C. Han, J. Yang, X. Zhang, A. Li and J. Peng, *CrystEngComm*, 2024, **26**, 203–208; (*g*) K. Chen, W. Wu, H. Zhao, Y. Wei, S. Zhu, X. Huang, N. Wang, T. Wang and H. Hao, *Cryst. Growth Des.*, 2023, **23**, 8637–8645; (*h*) B. B. Rath and J. J. Vittal, *Chem. Mater.*, 2021, **33**, 4621–4627; (*i*) S. Kusumoto, K. Wakabayashi, K. Rakumitsu, J. Harrowfield, Y. Kim and Y. Koide, *Chem. – Eur. J.*, 2024, e202401564; (*j*) J. Lin, J. Zhou, L. Li, I. Tahir, S. Wu, P. Naumov and J. Gong, *Chem. Mater.*, 2024, **36**, 8338–8348; (*k*) K. Chen, J. Wang, Y. Feng, H. Liu, X. Zhang, Y. Hao, T. Wang, X. Huang and H. Hao, *J. Mater. Chem. C*, 2021, **9**, 16762–16770; (*l*) Y.-S. Chen, C.-H. Wang, Y.-H. Hu, C.-Y. D. Lu and J.-S. Yang, *J. Am. Chem. Soc.*, 2023, **145**, 6024–6028; (*m*) P. Gupta, D. P. Karothu, E. Ahmed, P. Naumov and N. K. Nath, *Angew. Chem., Int. Ed.*, 2018, **57**, 8498–8502; (*n*) Y. Hao, L. Gao, X. Zhang, R. Wei, T. Wang, N. Wang, X. Huang, H. Yu and H. Hao, *J. Mater. Chem. C*, 2021, **9**, 8294–8301.

12 S. Ghosh and C. M. Reddy, *Angew. Chem.*, 2012, **124**, 10465–10469.

13 A. Worthy, A. Grosjean, M. C. Pfrunder, Y. Xu, C. Yan, G. Edwards, J. K. Clegg and J. C. McMurtrie, *Nat. Chem.*, 2018, **10**, 65–69.

14 M. K. Panda, S. Ghosh, N. Yasuda, T. Moriwaki, G. D. Mukherjee, C. M. Reddy and P. Naumov, *Nat. Chem.*, 2015, **7**, 65–72.

15 (*a*) A. J. Thompson, A. I. C. Orué, A. Jayamohanan Nair, J. R. Price, J. McMurtrie and J. K. Clegg, *Chem. Soc. Rev.*, 2021, **50**, 11725–11740; (*b*) Y. Funamori, R. Suzuki, T. Wakahara, T. Ohmura, E. Nakagawa and M. Tachibana, *Carbon*, 2020, **169**, 65e72; (*c*) P. Xu, B. Cui, Y. Bu, H. Wang, X. Guo, P. Wang, Y. R. Shen and L. Tong, *Science*, 2021, **373**, 187–192; (*d*) S. Hayashi, F. Ishiwari, T. Fukushima, S. Mikage, Y. Imamura, M. Tashiro and M. Katouda, *Angew. Chem., Int. Ed.*, 2020, **59**, 16195–16201; (*e*) S. P. Thomas, A. Worthy, E. Z. Eikeland, A. J. Thompson, A. Grosjean, K. Tolborg, L. Krause, K. Sugimoto, M. A. Spackman, J. C. McMurtrie, J. K. Clegg and B. B. Iversen, *Chem. Mater.*, 2023, **35**, 2495–2502; (*f*) S. Kusumoto, K. Oishi, M. Nakaya, R. Suzuki, M. Tachibana, Y. Kim, Y. Koide and S. Hayami, *CrystEngComm*, 2022, **24**, 8303–8308; (*g*) A. Sugimoto, S. Kusumoto, M. Nakaya, Y. Sekine, L. F. Lindoy and S. Hayami, *CrystEngComm*, 2022, **24**, 4656–4660; (*h*) S. Kusumoto, R. Suzuki, M. Tachibana, Y. Sekine, Y. Kim and S. Hayami, *Chem. Commun.*, 2022, **58**, 5411–5414; (*i*) S. Kusumoto, A. Sugimoto, Y. Zhang, Y. Kim, M. Nakamura, L. F. Lindoy and S. Hayami, *Inorg. Chem.*, 2021, **60**, 1294–1298; (*j*) S. Hayahi and T. Koizumi, *Chem. – Eur. J.*, 2018, **24**, 8507–8512; (*k*) M. K. Mishra and C. C. Sun, *Cryst. Growth Des.*, 2020, **20**, 4764–4769.

16 (*a*) L.-C. An, X. Li, Z.-G. Li, Q. Li, P. J. Beldon, F.-F. Gao, Z.-Y. Li, S. Zhu, L. Di, S. Zhao, J. Zhu, D. Comboni, I. Kupenko, W. Li, U. Ramamurty and X.-H. Bu, *Nat. Commun.*, 2022, **13**, 6645; (*b*) A. Mondal, B. Bhattacharya, S. Das, S. Bhunia, R. Chowdhury, S. Dey and C. M. Reddy, *Angew. Chem., Int. Ed.*, 2020, **59**, 10971–10980; (*c*) K. Naim, M. Singh, S. Sharma, R. V. Nair, P. Venugopalan, S. C. Sahoo and P. P. Neelakandan, *Chem. – Eur. J.*, 2020, **26**, 11979–11984; (*d*) X. Liu, A. A. L. Michalchuk, B. Bhattacharya, N. Yasuda, F. Emmerling and C. R. Pulham, *Nat. Commun.*, 2021, **12**, 3871; (*e*) L. O. Alimi, P. Lama, V. J. Smith and L. J. Barbour, *Chem. Commun.*, 2018, **54**, 2994–2997; (*f*) B. Bhattacharya, A. A. L. Michalchuk, D. Silbernagl, M. Rautenberg, T. Schmid, T. Feiler, K. Reimann, A. Ghalgaoui, H. Sturm, B. Paulus and F. Emmerling, *Angew. Chem., Int. Ed.*, 2020, **59**, 5557–5561; (*g*) S. Kusumoto, A. Sugimoto, D. Kosumi, Y. Kim, Y. Sekine, M. Nakamura and S. Hayami, *CrystEngComm*, 2021, **23**, 5560–5563; (*h*) S. Kusumoto, A. Saso, H. Ohmagari, M. Hasegawa, Y. Kim, M. Nakamura, L. F. Lindoy and S. Hayami, *ChemPlusChem*, 2020, **85**, 1692–1696.

17 (*a*) S. Takamizawa and Y. Miyamoto, *Angew. Chem., Int. Ed.*, 2014, **53**, 6970–6973; (*b*) S. Sakamoto, T. Sasaki, A. Sato-Tomita and S. Takamizawa, *Angew. Chem., Int. Ed.*, 2019, **58**, 13722–13726.

18 (*a*) T. Seki, C. Feng, K. Kashiyama, S. Sakamoto, Y. Takasaki, T. Sasaki, S. Takamizawa and H. Ito, *Angew. Chem., Int. Ed.*, 2020, **59**, 8839–8843; (*b*) S. H. Mir, Y. Takasaki, E. R. Engel and S. Takamizawa, *Angew. Chem., Int. Ed.*, 2017, **56**, 15882–15885.

19 S. Takamizawa, Y. Takasaki, T. Sasaki and N. Ozaki, *Nat. Commun.*, 2018, **9**, 3984.

20 (*a*) H. Koshima, N. Ojima and H. Uchimoto, *J. Am. Chem. Soc.*, 2009, **131**, 6890–6891; (*b*) O. S. Bushuyev, T. C. Corkery, C. J. Barrett and T. Friščić, *Chem. Sci.*, 2014, **5**, 3158–3164; (*c*) Y. Hao, S. Huang, Y. Guo, L. Zhou, H. Hao, C. J. Barrett and H. Yu, *J. Mater. Chem. C*, 2019, **7**, 503–508.

21 (*a*) D. J. van Dijken, P. Kovaříček, S. P. Ihrig and S. Hecht, *J. Am. Chem. Soc.*, 2015, **137**, 14982–14991; (*b*) B. Bai, M. Zhang, N. Ji, J. Wei, H. Wanga and M. Li, *Chem. Commun.*, 2017, **53**, 2693–2696.

22 (*a*) K. Uchida, S.-I. Sukata, Y. Matsuzawa, M. Akazawa, J. J. D. de Jong, N. Katsonis, Y. Kojima, S. Nakamura, J. Areephong, A. Meetsma and B. L. Feringa, *Chem. Commun.*, 2008, 326–328; (*b*) D. Kitagawa and S. Kobatake, *Chem. Commun.*, 2015, **51**, 4421–4424; (*c*) A. Hirano, T. Hashimoto, D. Kitagawa, K. Kono and S. Kobatake, *Cryst. Growth Des.*, 2017, **17**, 4819–4825; (*d*) R. Nishimura, A. Fujimoto, N. Yasuda, M. Morimoto, T. Nagasaka, H. Sotome, S. Ito, H. Miyasaka, S. Yokojima, S. Nakamura, B. L. Feringa and K. Uchida, *Angew. Chem., Int. Ed.*, 2019, **58**, 13308–13312.

23 (*a*) K. Yuhara and K. Tanaka, *Angew. Chem., Int. Ed.*, 2024, **63**, e202319712; (*b*) T. Nishiuchi, K. Kisaka and T. Kubo, *Angew. Chem., Int. Ed.*, 2021, **60**, 5400–5406; (*c*) K. Kato, T. Seki and H. Ito, *Inorg. Chem.*, 2021, **60**, 10849–10856.

24 (*a*) S. Khan, S. Naaz, A. Ekka, B. Dutta, S. Roy, R. Medishetty and M. H. Mir, *Chem. Commun.*, 2022, **58**, 12102–12105; (*b*) J. J. Vittal and H. S. Quah, *Dalton Trans.*, 2017, **46**, 7120–7140; (*c*) S. Kusumoto, K. Sato, K. Muraie, S. Masuda, K. Rakumitsu, Y. Kim and Y. Koide, *CrystEngComm*, 2023, **25**, 909–912; (*d*) S. Kusumoto, K. Sato, K. Rakumitsu, Y. Kim and Y. Koide, *Cryst. Growth Des.*, 2023, **23**, 8972–8977; (*e*) S. Kusumoto, K. Wakabayashi, K. Rakumitsu, Y. Kim and Y. Koide, *CrystEngComm*, 2024, **26**, 3791–3794; (*f*) B. B. Rath, M. Gupta and J. J. Vittal, *Chem. Mater.*, 2022, **34**, 178–185.

25 G. M. J. Schmidt, *Pure Appl. Chem.*, 1971, **27**, 647–678.

26 (*a*) C. J. Powell, E. Bosch, H. R. Krueger Jr and R. H. Groeneman, *New J. Chem.*, 2023, **47**, 13084–13087; (*b*) M. G. Vasquez-Rios, G. Campillo-Alvarado, D. C. Swenson, H. Hopfl and L. R. MacGillivray, *Chem. – Eur. J.*, 2022, **28**, e202104604; (*c*) S. P. Yelgaonkar, G. Campillo-Alvarado and L. R. MacGillivray, *J. Am. Chem. Soc.*, 2020, **142**, 20772–20777; (*d*) K. Tsaggeos, N. Masiera, A. Niwicka, V. Dokorou, M. G. Siskos, S. Skoulika and A. Michaelides, *Cryst. Growth Des.*, 2012, **12**, 2187–2194; (*e*) X. Gao, T. Friščić and L. R. MacGillivray, *Angew. Chem., Int. Ed.*, 2004, **43**, 232–236; (*f*) L. R. MacGillivray, J. L. Reid and J. A. Ripmeester, *J. Am. Chem. Soc.*, 2000, **122**, 7817–7818.